ISSN 0030-400X, Optics and Spectroscopy, 2008, Vol. 105, No. 1, pp. 134–140. © Pleiades Publishing, Ltd., 2008.
Original Russian Text © L.A. Ageev, K.S. Beloshenko, E.D. Makovetskiĭ, V.K. Miloslavskiĭ, 2008, published in Optika i Spektroskopiya, 2008, Vol. 105, No. 1, pp. 147–153.

LASERS AND THEIR APPLICATIONS

Observation of Radiation Instabilities of a Two-Mode He–Ne Laser with the Help of Interference of Polarized Rays

L. A. Ageev, K. S. Beloshenko, E. D. Makovetskiĭ, and V. K. Miloslavskiĭ

Karazin Kharkov National University, Kharkov, 61077 Ukraine

e-mail: Leonid.A.Ageev@univer.kharkov.ua

Received November 20, 2007

Abstract—Instabilities in the operation of a two-mode He–Ne laser are observed with the help of interference of polarized beams. Two interference patterns created by two radiation modes alternatively appear. The contrast of the interference pattern increases under the action of an external constant magnetic field on the laser. If one of the interfering beams is delayed sufficiently long, the instability manifests itself in the motion of interference fringes in a direction that depends on which of the two beams is delayed. The particular features of the evolution of the interference pattern are explained based on interference equations for the two modes that take into account the orthogonality of the linear polarizations of the modes, as well as changes in their amplitudes and frequencies.

PACS numbers: 42.55.Lt

DOI: 10.1134/S0030400X08070217

INTRODUCTION

Among various industrial continuous He–Ne lasers, there are lasers with a short isotropic passive cavity, which emit one or two axial modes. The cavity along with the active medium is considered to be quasi-isotropic, since the active medium is characterized by a dispersion of the refractive index in the amplification band, which leads to a difference in the refractive indices for different axial modes (the phase anisotropy). Practically, since the creation of lasers, numerous studies have been devoted to the study of the polarization of laser radiation. For example, the polarization under the single- and two-mode regimes was experimentally studied already in early works [1–3]; however, at present, the stability of generation, as well as of polarization, is also of interest [4]. It can be noted that, to denote the unstable polarization of laser beams, a new term, "random polarization," was coined in the reference literature on industrial lasers [5]. Our analysis of the literature devoted to the investigation of the polarization of beams of gas lasers showed that experimental investigations were performed using polarization [1–3] or spectral and polarization techniques [4]. At the same time, it has long been known that the radiation polarization can be efficiently studied using polarimeters whose action is based on interference of polarized beams [6].

In this study, we describe an optical scheme for obtaining polarized beams and present results of our observations of time evolution of interference related to amplitude, polarization, and frequency changes of modes.

OPTICAL SCHEME OF AN INTERFEROMETER

An interferometer for observing the interference of polarized beams is schematically shown in Fig. 1. A narrow beam (with a cross section of ~1 mm) emitted by a laser (*1*) passes through the center of a Wollaston prism (*2*) and is split into practically symmetric ordinary (*o*) and extraordinary (*e*) beams with an angle φ between them. We used a standard calcite Wollaston prism with a diameter of 17 mm and thickness of 5 mm, which ensures an angle of $\varphi \approx 1.7°$. After passing the prism, the ordinary and extraordinary waves are linearly polarized, with their polarizations being orthogonal to each other. A polaroid (*3*) was assembled in a common holder with the Wollaston prism such that the plane of polarization of the polaroid would make an angle of 45° with the orthogonal optical axes of the prism. After passing the polaroid, the polarizations of the two beams lie in its polarization plane. Both the Wollaston prism and the polaroid are arranged such that the angle of incidence of the laser beam on their plane faces would slightly differ from zero and the beams reflected by the faces would miss the cavity. After the polaroid, the two beams symmetrically pass through a collecting lens (*4*) (with the focal plane (*5*)) and intersect each other at an angle α in the vicinity of the point *O*. The distance *b* between the lens center and point *O* can be found from the thin lens formula. We used a lens with a focal distance of $f = 11$ cm, which was placed at a distance of $a \approx 27$ cm from the center of the Wollaston prism; in this case, $b = 18.6$ cm, and the angle of convergence of the beams to the point *O* is $\alpha \approx 2.4°$.

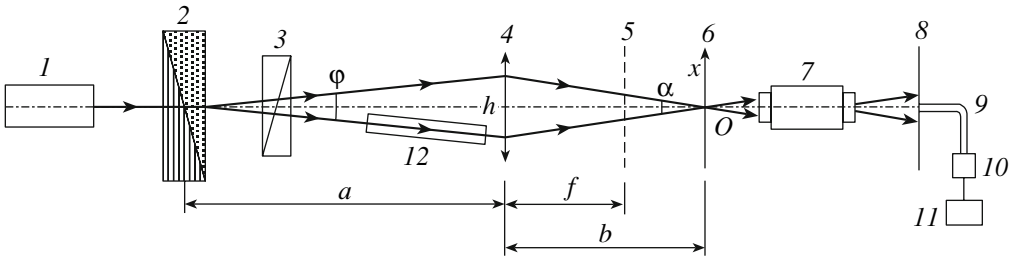

Fig. 1. Optical scheme for observation of interference of polarized beams: (*1*) laser, (*2*) Wollaston prism, (*3*) polaroid, (*4*) lens, (*5*) focal plane of the lens, (*6*) plane of observation of interference, (*7*) microscope, (*8*) screen, (*9*) optical fiber, (*10*) PMT, (*11*) microammeter, and (*12*) delay line. In the scheme, *a* is the distance between the Wollaston prism and the lens; *f* is the focal distance of the lens; *h* is the distance between the beams on the lens; *b* is the distance from the lens to the point *O* of intersection of the beams in plane *6*; φ is the divergence angle of the two beams emerged from the Wollaston prism; α is the convergence angle of the interfering beams; *X* is the coordinate in plane *6*; and *O* is the coordinate origin.

The interference pattern is observed in a plane (*6*) that passes through the point *O* and is perpendicular to the bisectrix of the angle α. Interference fringes are formed in this plane in the intersection area of the beams. These fringes are perpendicular to the *X* axis, whose origin is at the point *O* and which is formed by the intersection of plane *6* and the plane containing the convergent beams. The wave vector **K** of the interference pattern is parallel to the *X* axis and is equal to the difference $\mathbf{K} = \mathbf{k}_1 - \mathbf{k}_2$, where $\mathbf{k}_{1,2}$ are the wave vectors of the beams. The modulus of the vector **K** is $K = 2k_x$, where $k_x = (2\pi/\lambda)\sin(\alpha/2)$ are the projections of $\mathbf{k}_{1,2}$ onto the *X* axis. The period $\Lambda = 2\pi/K$ of the interference pattern is given by

$$\Lambda = \lambda/[2\sin(\alpha/2)]. \quad (1)$$

For the radiation of the He–Ne laser at $\lambda = 632.8$ nm and for the angle $\alpha \approx 2.4°$, we find $\Lambda \approx 15$ μm. A pattern with such a period is indistinguishable to the unaided eye and, to observe it, we used a horizontal microscope (*7*) with an objective ($8^{\times}$) and an ocular ($10^{\times}$). Since the brightness of the laser beam is high, the interference pattern was not observed directly via the ocular but was projected by the ocular onto a screen (*8*). The focusing procedure of the microscope to observe the pattern was simple. The objective was placed behind plane *6* at a distance that is approximately equal to the focal distance of the objective. If the focusing is inexact, two separated light spots from the two beams are seen on the screen. In this case, the drawtube is displaced along the optical axis until the two spots completely superimpose each other. As a result, interference fringes are observed on the entire area of the common spot of the beams. Screen *8* can be placed at various distances from the ocular. With increasing distance, the period of the interference pattern on the screen linearly increases because of the angular magnification of the microscope. In our experiments, the screen was placed at a distance of ≈1.5 m; the period of the pattern was ≈0.7 cm; and approximately 25 fringes were observed within the area of the entire spot. The same number of fringes should be observed in the light spot formed by the intersecting beams in plane *6*. Since $\Lambda \approx 15$ μm in this plane, the maximal diameter of the spot of the intersecting beams is about 0.4 mm.

Screen *8* was made of a high-quality semitransparent paper, so that the pattern can be observed on both sides of the screen. The intensity of the fringes in the pattern was photoelectrically measured by an optical fiber with a diameter of 2 mm placed right up to the backside of the screen. The fiber sent the light from the pattern to a photomultiplier, and the corresponding electric signal was measured with a microammeter. The interference pattern was also recorded with a digital video camera installed behind the screen.

RESULTS OF OBSERVATIONS

In this paper, we studied the radiation of an LGN-208A two-mode He–Ne laser. The main results were obtained within approximately 0.5 h after the laser was switched on.

First of all, it should be noted that we indeed observed the interference pattern but it was unstable in time. Especially rapid changes occurred immediately after the switching-on of the laser. These changes gradually slowed down, and certain fragments in the pattern were observed within longer and longer time intervals. At the same time, the basic features of the pattern were retained throughout the period of time of continuous observations. These features are as follows: initially, an interference pattern is observed (Fig. 2a); then, it becomes less and less visible until it completely vanishes (Fig. 2b), and a new pattern arises (Fig. 2c), which is opposite to the preceding pattern in that its maxima exchange places with the minima of the preceding pattern. That is, the first and the second patterns are antipodes of each other. Then this process is repeated in the reversed order, and the two patterns are alternately observed throughout the entire period of observations, with the stages described above being observed within longer and longer time intervals.

The unstable interference was also detected by the photoelectric method. The input end of the optical fiber

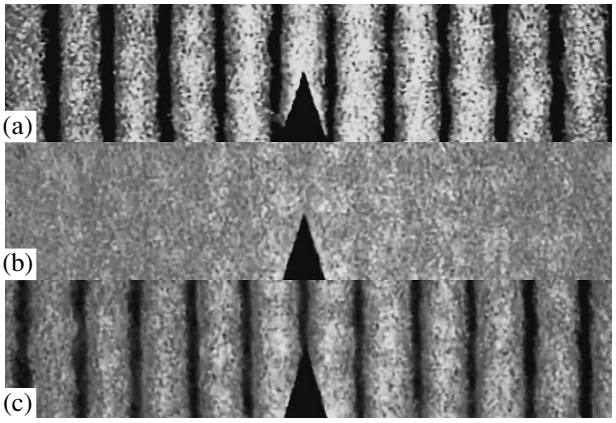

Fig. 2. Basic evolution stages of interference: (a) interference pattern observed at a certain time instant, (b) vanishing of the interference pattern at a subsequent moment, and (c) antipodal interference pattern.

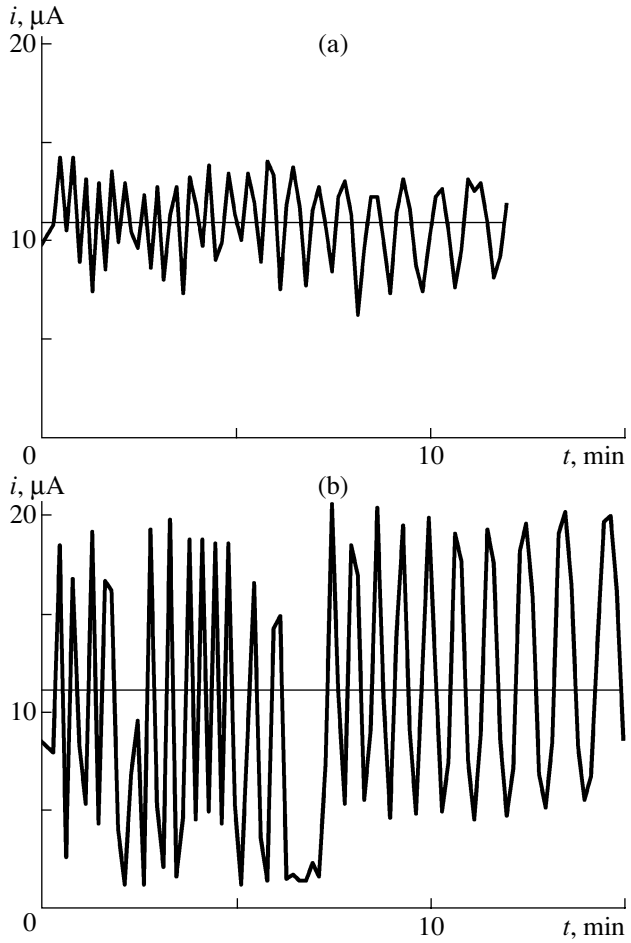

Fig. 3. Irregular intensity oscillations in an interference pattern: (a) without a magnetic field and (b) in a magnetic field. Solid lines are the average values of the relative intensity over the entire measurement time.

was fixed such that it received light from an interference extremum at the moment of the best visibility of the interference pattern. The electric signal was measured at intervals of 10 seconds for 12 min. The results of these measurements are shown in Fig. 3a. It is seen that the measured intensity irregularly oscillates. The maxima correspond to moments when the fiber receives the light from the interference maxima of one of the two interference patterns, and the minima correspond to the interference minima from the second (antipodal) pattern. The ratio of the averaged values of I_{min}/I_{max} yields the average visibility of the interference $V = (1 - I_{min}/I_{max})/(1 + I_{min}/I_{max}) \approx 0.2$. The horizontal line corresponds to the average relative intensity determined over the measurement time. The points of intersection of this line with the oscillating curve approximately correspond to moments when the interference pattern completely vanishes. The oscillations are irregular in both amplitude and frequency. It is clearly seen that the frequency of oscillations gradually decreases with time.

It is well known that a magnetic field significantly affects the oscillation of gas lasers. In our experiments, we studied this effect by a simplest method. A permanent magnet made of barium ferrite in the form of a plate, $8 \times 4 \times 1.5$ cm in size, was put on the middle part of the laser casing, with the long side of the magnet being parallel to the laser axis. The plane of the magnet was at a distance of about 2 cm from the axis of the laser tube. The field strength created by the magnet at this distance was 200 Oe.

Under the action of the field, the visibility of the interference was significantly increased. The behavior in time of other features of the pattern was unaffected. The changes in the intensity photoelectrically measured within 15 min are shown in Fig. 3b. According to these data, the average interference visibility reaches a value of $V \approx 0.7$. As in the absence of the field (Fig. 3a), the frequency of oscillations decreases with time. Note that Fig. 2 corresponds to interference patterns observed in the presence of the magnetic field and is a sequence of freeze-frames from the video recording.

Our observations of the interference behavior within long time periods (longer than an hour) after the laser was switched off showed that an interference pattern can be retained unchanged for a long time (about 10 min); then, randomly, a comparatively short stage (about 1 min) occurs during which the interference pattern becomes blurred and vanishes. After that, the opposite pattern arises, which is equally stable as the preceding pattern.

Such a behavior of the interference considerably changes if a delay line (*12* in Fig. 1) is introduced into one of the two beams. Since the frequencies of the two modes are close to each other, for changes to be appreciable, the delay should be long. In our experiments, we used a cylindrical ruby rod with polished ends (an active element of a ruby laser), whose diameter was 12 mm and length was 117 mm. On passage through the rod, the laser beam was not distorted, which indi-

cates that the ruby crystal used was highly optically homogeneous. The optical axis of the ruby rod makes an angle with the rod axis; therefore, the rod polarizes the light passing through it. When introducing into the beam, the rod was rotated about its axis such that the polarization of the passed beam would remain the same. The intensity of the passed beam decreased insignificantly since ruby is transparent at $\lambda = 632.8$ nm. The refractive index of ruby is $n = 1.76$.

Upon introduction of the ruby rod into the scheme, the interference visibility significantly increased, which was especially seen in the absence of the magnetic field. The interference pattern never vanished, and only small irregular changes in the visibility were observed. The interference pattern moves as a whole in a certain direction along the X axis. The rate of this motion was maximal immediately after the laser was switched on; then, the rate gradually decreased. Upon placing the ruby rod into the second beam, the motion of fringes reverses. In a sufficiently long period of time (~1 h) after switching-off the laser, the continuous motion of fringes ceases; however, it can occur within short uncontrolled time periods.

DISCUSSION OF RESULTS

Before discussion of the results, we will present the published data on the radiation of an LGN-208A laser [3, 4]. This laser emits a TEM_{00} beam with an average wavelength of $\lambda = 632.8$ nm. The beam contains two axial modes, whose linear polarizations are orthogonal to each other. The frequency interval between the modes is $\Delta\nu_a = C/2L = 640$ MHz (C is the speed of light in the active medium, $L \approx 23.4$ cm is the cavity length). The spectral width of the mode can be estimated from the formula $\delta\nu \approx \Delta\nu_a(1 - r)/\pi$, where r is the reflection coefficient of the cavity mirror. For $r \approx 0.99$, we find that, on the order of magnitude, $\delta\nu \sim 1$ MHz. The inhomogeneous (Doppler) width of the amplification band is $\Delta\nu_D \approx 1400$ MHz [7]. Upon scanning the modes over the amplification band, the polarization plane is rotated by 90° as the mode passes through the band center (the Lamb dip) [8, 9]. The instability of modes in frequency, amplitude, and polarization is determined by many factors such as thermal and mechanical deformations of the cavity, the influence of external magnetic fields, including the Earth's magnetic field [4, 10], inhomogeneities and instabilities of the gas discharge, and so on.

All this shows that the results of our observations should be discussed taking into account the two-mode lasing regime, the orthogonal linear polarizations of the modes and the shift of the modes over the amplification band under the action of external factors. We will denote the modes by the figures 1 and 2. The modes are independent of each other, have different frequencies $\nu_{1,2}$, a small width $\delta\nu$, and are spaced from each other by $\Delta\nu_a \gg \delta\nu$. Hence, each mode should create its own interference pattern. Let A_1 and A_2 be the initial amplitudes of the modes (Fig. 4). The arrows in this figure show the orthogonal directions of the mode polarizations. After passing through the Wollaston prism, the oscillations of the ordinary and extraordinary components of modes 1 and 2 are denoted, respectively, as e_1, o_1 and e_2, o_2. The projections of these oscillations onto the polarization direction PP of the polaroid are denoted, respectively, as e_1', o_1' and e_2', o_2'. Interference arises upon addition of oscillations o_1' and e_1' of mode 1 and upon addition of oscillations o_2' and e_2' of mode 2. Figure 4 shows that the oscillations of modes 1 and 2 are shifted in phase by π.

The Wollaston prism of the interferometer of Fig. 1 practically does not create a path length difference for beams emerging from it. Also, we assume that beams do not acquire a path length difference upon passage through the polaroid and lens. Therefore, the interference is created by symmetric beams emerging from the lens. In the absence of a delay line, the path length difference of these beams at the point O in plane *6* is zero; consequently, this point is the center of the interference. Upon displacement along the X axis, one observes alternating interference extrema of the mth order ($m > 0$). A phase difference $\psi = KX = 2k_xX$, which depends on the coordinate X, corresponds to these extrema. We will assume that, for mode 1, the interference is determined by this phase difference, whereas, for mode 2, it should differ by π (Fig. 4).

Therefore, in accordance with the geometry of Fig. 4, the intensities I_1 and I_2 in the interference equations for modes 1 and 2 are written as

$$\begin{aligned} I_1 &= A_1^2(1 + \cos 2\varepsilon \cos\psi)/2, \\ I_2 &= A_2^2(1 - \cos 2\varepsilon \cos\psi)/2. \end{aligned} \tag{2}$$

Consequently, two interference patterns are formed in observation plane *6*, whose addition yields the resultant intensity distribution

$$\begin{aligned} I &= I_1 + I_2 \\ &= [A_1^2 + A_2^2 + (A_1^2 - A_2^2)\cos 2\varepsilon \cos\psi]/2. \end{aligned} \tag{3}$$

The gradual heating of the laser after its switching-on and the change in the cavity length L caused by this heating should be considered to be the main factors that determine the motion of the modes in the amplification band. This is a slow process, since the heat source is a thin gas discharge, while the thermal energy is spent for heating comparatively massive accessories and mounting elements. As L changes with temperature, the modes are shifted over the amplification band, with their amplitudes A_1 and A_2 also changing. At the same time, the azimuths ε and $\varepsilon + \pi/2$ (Fig. 4) of the orthogonal polarizations of the modes can remain unchanged for a long time [3]. In this case, it is possible to adjust the scheme of Fig. 1 such that the interference visibility

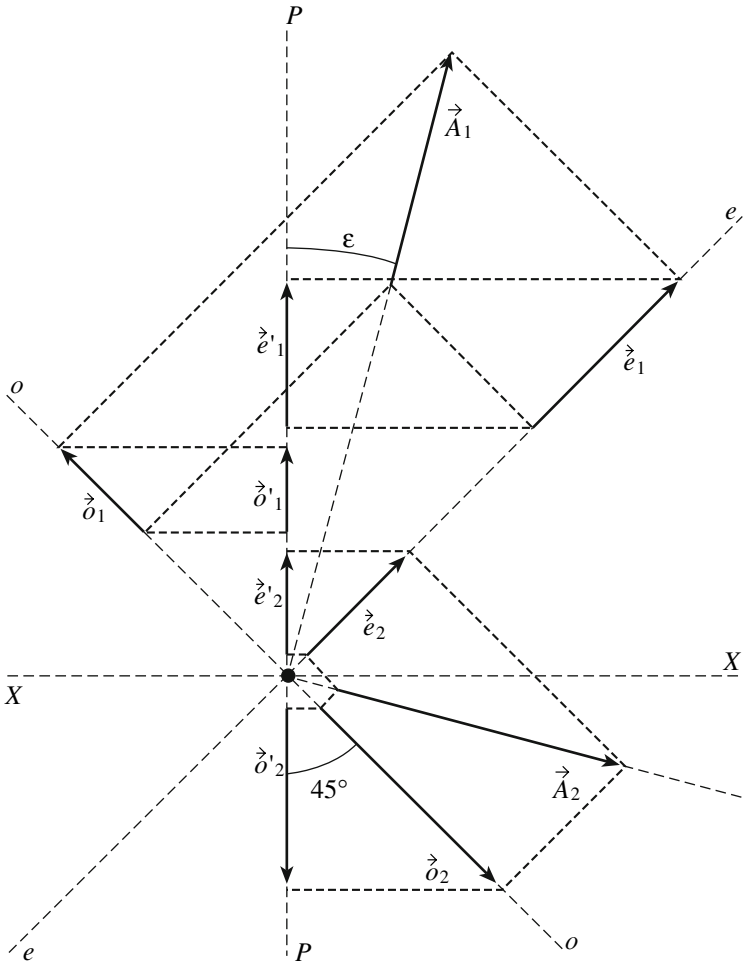

Fig. 4. Scheme of transformations of mode oscillations in a Wollaston prism and polaroid: A_1 and A_2 are the amplitudes of orthogonal oscillations in modes 1 and 2; ε is the azimuth of these oscillations; e_1, o_1, e_2, and o_2 are the projections, which determine oscillations at the output from the Wollaston prism; e'_1, o'_1, e'_2, and o'_2 are the projections onto the polarization direction *PP* of the polaroid, which determine oscillations in interfering beams.

would be maximal. Then, one can set $\cos 2\varepsilon = 1$ in expression (3). In this case, the interference will occur at $A_1 \neq A_2$ and will vanish at $A_1 = A_2$. If $A_1 \gg A_2$, the positions of extrema in the resultant pattern correspond to their positions in the pattern created by mode 1 alone. Conversely, if $A_1 \ll A_2$, the resultant pattern coincides with the pattern created by mode 2 alone, i.e., becomes antipodal with respect to the preceding pattern. The equality of amplitudes and vanishing of the interference connected with it occur within comparatively short time periods when the positions of the modes are symmetric with respect to the center of the amplification band. For this reason, the time intervals of the interference vanishing are noticeably shorter than the intervals of occurrence of the interference patterns.

To comprehensively analyze the behavior of the interference in the presence of a delay line, it is necessary to take into account in formulas (2) and (3) the path difference $(n - 1)s$ (n is the refractive index of the medium of the delay line, s is the delay line length) introduced by the delay line, as well as the difference between the frequencies ν_1 and ν_2 of the modes and changes in these frequencies upon shift of the modes within the amplification band. Then, the phase differences in Eqs. (2) for modes 1 and 2 should be written as

$$\psi_{1,2} = 2\pi\nu_{1,2}[2X\sin(\alpha/2) \pm (n-1)s]/C. \qquad (4)$$

The "+" and "–" signs correspond to the cases where the delay line is placed in one or the other beam (Fig. 1).

Formulas (2) and (4) allow one to clarify how the delay line will affect the visibility of the interference. For definiteness, we take in calculations the plus sign in (4) and set $A_1 = A_2$, $\cos 2\varepsilon = 1$, $\nu_1 = \nu_0 - \Delta\nu_a/2$, $\nu_2 = \nu_0 + \Delta\nu_a/2$, $\nu_0 = C/\lambda_0$, $C = 3 \times 10^{10}$ cm/s, $\lambda_0 = 6.328 \times 10^{-5}$ cm, and the frequency interval between the modes $\Delta\nu_a = 6.4 \times 10^8$ s^{-1}. The calculations were performed in

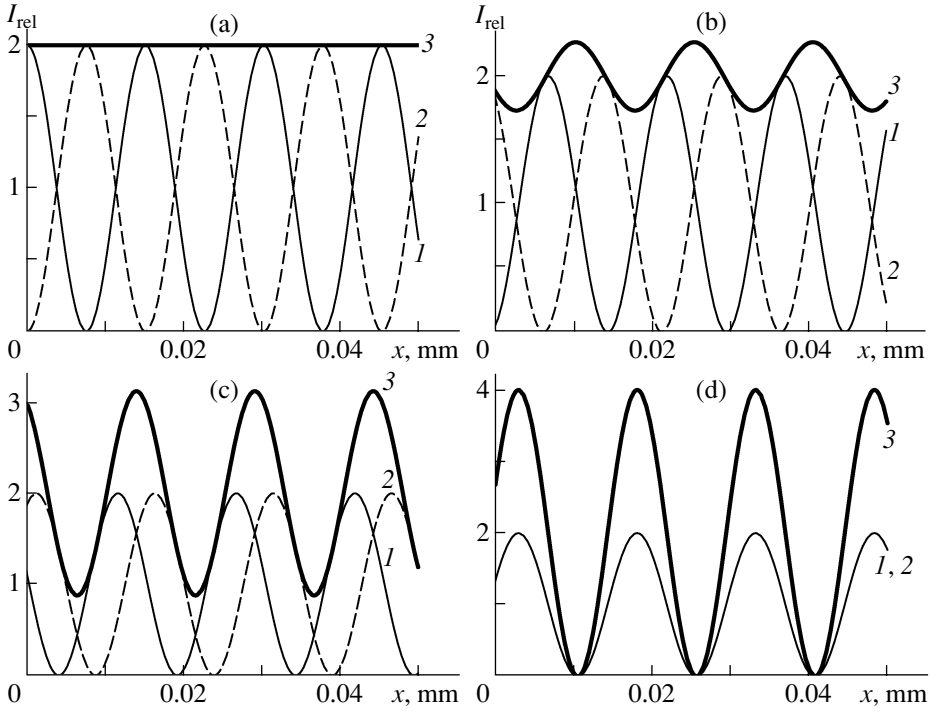

Fig. 5. Interference patterns calculated for different values of the path difference introduced by a delay line: $(n-1)s$ = (a) 0, (b) 20, (c) 88.92, and (d) 234 mm. Curves: (*1*) interference pattern of mode 1, (*2*) interference pattern of mode 2, and (*3*) total interference pattern.

the interval $0 \le X \le 0.05$ mm for four values of the path difference $(n-1)s$ = 0, 20, 88.92, and 234 mm introduced by the delay line. The value 88.92 mm corresponds to the path difference introduced by the ruby rod; the path difference 234 mm is equal to the cavity length of the laser. The calculation results are presented in Fig. 5. It is seen that, in the absence of the delay line, the interference patterns created by the two modes are antipodal and completely cancel each other (Fig. 5a). If the delay line introduces a comparatively small path difference (Fig. 5b), the resultant interference pattern at $A_1 = A_2$ no longer vanishes but its visibility is low. If the path difference introduced is long (ruby, Fig. 5c), the visibility becomes sufficiently high ($V > 0.5$). Finally, if the difference introduced by the delay line is equal to the cavity length (Fig. 5d), the two interference patterns coincide (they are in consonance with each other), and the visibility reaches a value of $V = 1$. We note that it is difficult to realize the condition of coincidence; for example, to satisfy this condition, a perfect ruby crystal with a length of s = 308 mm is required. At the same time, such an interference consonance corresponds to the beat frequency of the two modes that can be easily observed with the help of a radiofrequency spectrum analyzer with a ferroelectric detection of the laser beam [4].

Finally, we will explain the experimentally observed motion of the interference pattern and the reversal of this motion as the delay line is transferred from one beam to the other. The motion of the pattern should be related to the shift of the modes within the amplification band as a result of a thermal elongation of the cavity. For the constant frequency interval $\Delta\nu_a$ between the modes, the motion of extrema of a resultant pattern will correspond to the motion of extrema in the pattern created by one mode alone. For the analysis, we will choose mode 1. For simplicity, we will omit the index in the notation of the frequency (wavelength) of this mode. It follows from expression (4) that the interference maximum of the mth order is defined by the condition

$$2\pi\nu(t)[2X_m(t)\sin(\alpha/2) \pm (n-1)s]/C = 2m\pi, \quad (5)$$

where t is the time. This condition shows that the rate of the displacement of the mth maximum is proportional to the rate of the shift of the frequency of the mode. Within the time period Δt, the maximum is displaced by

$$\Delta X_m = -(\Delta\nu/\nu)[X_m \pm (n-1)s/2\sin(\alpha/2)], \quad (6)$$

where $\Delta\nu$ is the frequency shift of the mode during the period Δt. By setting $X_m = 0$ in (6), we find that the maximum is displaced toward positive or negative values of the coordinate X depending on in which of the two interfering beams the delay line was placed. The displacement depends on the length s of the delay line, and, at $s = 0$, the interference pattern formed by the chosen mode, in agreement with experiment, becomes sta-

ble. Using the same condition ($X_m = 0$) and taking into account relation (1), we can express displacement (6) in terms of the period of interference Λ as

$$\Delta X_m = \mp(n-1)s\Delta\nu\Lambda/C. \quad (7)$$

Based on (7), we can estimate ΔX_m. We will use the following values of the path difference introduced by the delay line: $(n-1)s = 88.92$ and 234 mm and set $\Delta\nu = \Delta\nu_D = 14 \times 10^8$ s^{-1}. As a result, we find that $|\Delta X_m| \approx 0.41\Lambda$ and 1.09Λ, respectively. That is, as the mode is shifted within the entire amplification band, the mth maximum is displaced by almost a half of the period Λ in the first case and by more than this period in the second case. The continuity of the motion of extrema of the interference pattern is connected with the fact that as one mode passes through the entire range of the amplification band, the next mode falls into this range, etc., and this continues until the cavity length L becomes stabilized in value.

CONCLUSIONS

The advantage of the considered scheme of interference of polarized beams based on the Wollaston prism is that this scheme allows one to observe the interference pattern in a vicinity of the zero path difference of interfering beams. It is this specific feature of the scheme that makes it possible to observe the nonstationarity of oscillation of the considered two-mode laser, which manifests itself in a characteristic time evolution of the interference pattern, caused by the shift of modes over the amplification band and by stepwise changes in their polarization.

The variant of the scheme where a delay line placed in one of the interfering beams introduces a long path difference makes it possible to observe interference of high orders m and the motion of the interference pattern under the transient oscillation regime. This motion is connected with the rate of shift of modes over the amplification band.

Due to these particular features of the scheme proposed, the oscillation stability can be studied not only in gas lasers but also in other lasers with short cavities.

ACKNOWLEDGMENTS

This work was supported by the national budget of Ukraine (project no. DR 0107U008294).

REFERENCES

1. J. Kannelaud and W. Culshaw, Phys. Rev. **141** (1), 237 (1966).
2. E. Yu. Andreeva, D. K. Terekhin, and S. A. Fridrikhov, Opt. Spektrosk. **27**, 809 (1969).
3. A. N. Vlasov, V. A. Perebyakin, S. Yu. Polyakov, and V. E. Privalov, Kvantovaya Élektron. (Moscow) **13** (2), 320 (1986).
4. G. L. Kononchuk and V. V. Stukalenko, Ukr. Fiz. Zh. **48** (3), 417 (2003).
5. Melles Griot Catalog 1997, pp. 517–518.
6. P. P. Feofilov, *The Physical Basis of Polarized Emission: Polarized Luminescence of Atoms, Molecules, and Crystals* (Fizmatgiz, Moscow, 1959; Consultants Bureau, New York, 1961).
7. O. Zvelto, *Principles of Lasers* (Plenum, New York, 1989; Mir, Moscow, 1990).
8. W. Van Haeringen, Phys. Rev. **158** (2), 256 (1967).
9. A. S. Lipatov and V. N. Parygin, Kvantovaya Élektron. (Moscow) **5** (10), 2098 (1978).
10. V. G. Gudelev and V. M. Yasinskiĭ, Kvantovaya Élektron. (Moscow) **9** (7), 1420 (1982).

Translated by V. Rogovoĭ